Response to Reviewers

Referee #1

The manuscript "Seasonal variation of oxygenated organic molecules in urban Beijing and their contribution to secondary organic aerosol" addresses the seasonality of oxygenated organic molecules (OOM) in urban Beijing measured by a nitrate-CIMS over one year. And their potential contributions to secondary organic aerosol (SOA) via vapor condensation were estimated using an aerosol dynamic model. OOM concentrations were found to be highest in summer and generally followed the trend of radiation and temperature. OOM were classified into IP-OOM, MT-OOM, aromatic and aliphatic OOM. IP-OOM concentration vary strongly among seasons with lowest concentration in winter. Isoprene-OOM accounted for a large fraction in summer while in other seasons aromatic and aliphatic-OOM were the two major components. MS Profile of MT-OOM, aromatic and aliphatic OOM were similar among different seasons. Condensation of aromatic- and aliphatic-OOM contributed most to SOA throughout the year. Observation OOMs in urban environment are important to elucidate the SOA formation and particle growth but are scare as most field observations of OOMs were conducted in forested regions. Especially long time observation regarding seasonality of OOM is lacking. This study investigated one-year OOM compositions and concentrations systematically, which provides very valuable information of OOM seasonality and potential contribution to SOA. The manuscript is well written and fits well with the scope of ACP. I recommend its publication after addressing the following comments, which mainly work to clarify some important details and improve the readability and discussion of the manuscript.

We thank the reviewer for the constructive comments and suggestions. And as suggested, we added more details and modified corresponding descriptions to make our analysis easier to follow. The point-to-point response to the comments is given below. And the comments, our replies, and the corresponding changes in the revised manuscript and supplementary information are marked in black, blue, and green texts, respectively.

Specific comments

1. L60, I suggest explicitly mentioning the definition of OOM.

Response: Thanks a lot and this is really necessary.

The terminology OOMs comes from the term HOMs (Highly Oxygenated Organic Molecules), which is defined based on three criteria (Bianchi et al., 2019): a. HOMs are formed via autoxidation involving peroxy radicals, b. HOMs are formed in the gas phase under atmospherically relevant conditions, and c. HOMs typically contain six or more oxygen atoms. However, when looking into the oxygenated organic molecules measured at urban Beijing, the criteria of a. and c. are not always met. For example, in the oxidation processes, precursor VOCs may undergo multi-generation oxidation (Zaytsev et al., 2019;Garmash et al., 2020) and the autoxidation is sometimes suppressed by high NO_x level. This leads to the fact that not all organic molecules measured by the nitrate CIMS contain six or more oxygen atoms (see Fig. S7). This is the reason why we don't use the term HOMs.

OOMs is a more general terminology that refers to the gas phase organic compounds which are formed via oxidation process under atmospheric conditions. Thus, the guidelines for the classification of OOMs should be:

a. OOMs are the gas-phase oxygen-containing organic molecules detected under atmospherically relevant conditions.

b. OOMs can be formed via oxidations in the gas phase, heterogeneous reactions on aerosol surface, or evaporated processes from aerosols.

The definition of OOMs has been explicitly explained in a recent work by Nie et al. (Nie et al., 2022). Therefore, we added this paper as a reference of this sentence and explain the definition in more details in Sect. S2 (Line 22 – 35, Page 2).

"oxygenated organic molecules (OOMs, see the definition in Sect. S2 the work of Nie et al. (Nie et al., 2022)) have been acknowledged as an important contributor" (Line 59 – 60, Page 3)

2. In this study only m/z 200-400 was analyzed. Why other m/z, such as higher m/z were not included? What about their contributions? Are they too low to be important? It would be worth clarifying and noting the m/z range in the conclusion.

Response: We didn't report OOMs with higher m/z primarily because peaks in this range are very weak. Please note that those weak signals are not due to the transmission of the instrument, which remain roughly 94 % for m/z 400-680 range relative to that in the m/z 200-400 range. Rather, the low signal at higher m/z suggests that compounds of these masses are in very low concentrations. According to previous studies, the peaks with m/z larger than 400 are usually C_{15}-C_{20} compounds. They can either be the products from the dimeric reactions of monoterpenes (Ehn et al., 2012;Jokinen et al., 2014;Yan et al., 2016), or the oxidations of larger VOCs, such as sesquiterpene and diterpenes (Richters et al., 2016;Luo et al., 2022). However, in our studied urban environment, the concentrations of sesquiterpene and diterpenes are very low, and the formation of dimeric compounds is greatly suppressed by high-level NO_x. Therefore, the low signal at m/z > 400 can be well expected.

Meanwhile, we do observe some peaks at m/z > 400 range, but they are likely fluorine-containing contaminants and irrelevant to ambient processes. For example, the signal at m/z = 427 is mainly contributed by $(C_3F_7COO)_2H^-$ and the isotope of $C_6H_{13}COOH{\bullet}NO_3^-$, and remaining OOM signals are quite low (Fig. R1). The weak OOM signals together with the prominent contaminant signals make accurate peak identification difficult. Therefore, we decided not to focus too much on the higher m/z range, which nevertheless, has little influence on the conclusion of this study.

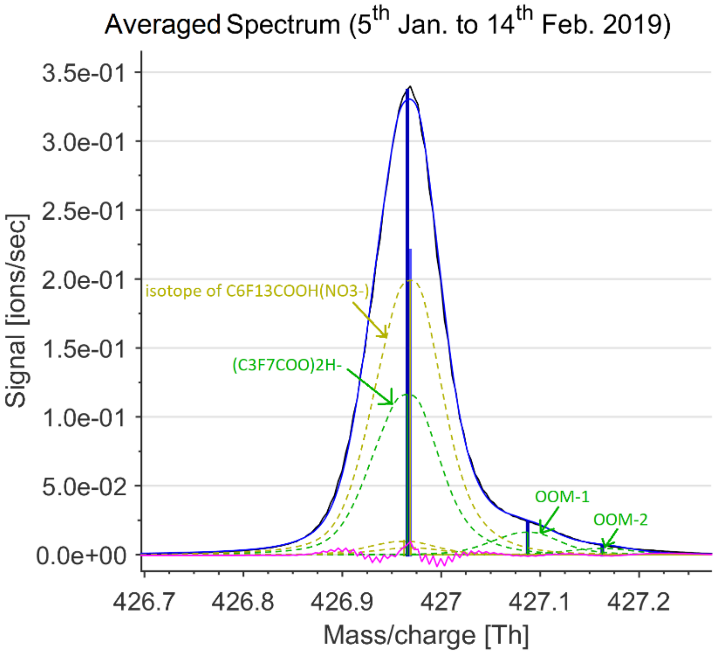

Figure R1. Fitted peaks at m/z = 427 Th of averaged winter spectrum (5th Jan. to 14th Feb., 2019).

For OOMs with m/z lower than 200 Th, their real molar weight after subtracting reagent ions should be low. Thus, they are generally more volatile and are not important to the condensational growth of SOA. One of the aim of this study is to investigate the SOA growth caused by OOM condensation, and this is the main reason why "light OOMs" are not included.

To clarify this consideration, we added the mass range of OOMs in the revised conclusion part as follows:

"A long-term measurement of OOMs based on nitrate CIMS was conducted in urban Beijing. OOMs in the mass range of 200-400 Th were systematically investigated." (Line 494 – 495, Page 21)

3. In the method part (L173, Fig. 1), it seems that the authors used a IP-OOM list to differentiate whether a compound belongs to IP-OOM. It may be helpful to include the list and describe what experiments/observations the list is based on.

Response: Thanks a lot for your suggestion. This isoprene OOM list is taken from the work of Xu et al. (Xu et al., 2021), where multifunctional products of isoprene oxidation were observed in both Nanjing and Shanghai. In this study, based on the molecular composition of precursor isoprene as well as current knowledge of atmospheric isoprene oxidation, the authors were able to constrain the double bond equivalence, numbers of hydrogen and number of effective oxygen of isoprene oxidation products. And according to those constrains, isoprene OOM molecules were selected.

We also added the isoprene OOM list in the revised supplement as Table S6.

Table S6. Peak list of isoprene OOMs in this study based on the work of Xu et al. (Xu et al., 2021)

Molecular Formula	Exact Mass
CHO	
$C_4H_6O_4(NO_3^-)$	180.0150
$C_5H_8O_4(NO_3^-)$	194.0306
$C_5H_8O_5(NO_3^-)$	210.0255
$C_4H_6O_6(NO_3^-)$	212.0048
$C_5H_{10}O_5(NO_3^-)$	212.0412
$C_4H_8O_6(NO_3^-)$	214.0205
$C_5H_{12}O_5(NO_3^-)$	214.0568
$C_5H_8O_6(NO_3^-)$	226.0205
$C_5H_{10}O_6(NO_3^-)$	228.0361
$C_4H_8O_7(NO_3^-)$	230.0154
$C_5H_{12}O_6(NO_3^-)$	230.0518
$C_5H_8O_7(NO_3^-)$	242.0154
CHON	
$C_5H_9O_4N(NO_3^-)$	209.0415
$C_4H_7O_5N(NO_3^-)$	211.0208
$C_5H_9O_5N(NO_3^-)$	225.0364
$C_4H_7O_6N(NO_3^-)$	227.0157
$C_5H_9O_6N(NO_3^-)$	241.0314
$C_4H_7O_7N(NO_3^-)$	243.0106
$C_5H_{11}O_6N(NO_3^-)$	243.0470
$C_5H_9O_7N(NO_3^-)$	257.0263
$C_5H_{11}O_7N(NO_3^-)$	259.0419
$C_5H_9O_8N(NO_3^-)$	273.0212
$C_4H_7O_9N(NO_3^-)$	275.0004
$C_5H_{11}O_8N(NO_3^-)$	275.0368
$C_5H_{11}O_9N(NO_3^-)$	291.0317
$C_5H_9O_{10}N(NO_3^-)$	305.0110
$CHON_{2,3}$	

$C_5H_{10}O_6N_2(NO_3-)$	256.0423
$C_4H_8O_7N_2$ (NO_3-)	258.0215
$C_5H_{10}O_7N_2(NO_3-)$	272.0372
$C_5H_{10}O_8N_2(NO_3-)$	288.0321
$C_5H_{10}O_9N_2(NO_3-)$	304.0270
$C_4H_8O_{10}N_2(NO_3-)$	306.0063
$C_5H_{10}O_{10}N_2$ (NO_3-)	320.0219
$C_5H_9O_{10}N_3(NO_3-)$	333.0172

4. Also in this part and Fig. 3, have the authors considered the possible contribution of isoprene to C10-OOM via accretion reactions and contribution of monoterpene to C5-OOM via fragmentation?

Response: We didn't incorporate the C5 OOMs formed from monoterpene (MT) fragmentation, nor the C10 OOMs formed from isoprene (IP) accretion in the workflow. This can result in some uncertainties, which however, are expected to be quite low.

As aforementioned, the list of IP oxidation products was taken from the work of Xu et al. (Xu et al., 2021), where all the IP OOMs are either C_4 or C_5 compounds. It has shown in chamber studies that via RO_2 cross reactions, isoprene oxidation can lead to the formation of C10 dimeric products (Bernhammer et al., 2018;Wu et al., 2021), yet such RO_2 cross reaction is severely suppressed by the high-level NO_x (up to 9.5 – 38.3 ppb) in Beijing, limiting the formation of C10 isoprene products. Therefore, the C10 OOMs generated from isoprene are neglected in the workflow.

In previous experiments conducted in the CLOUD chamber, monoterpene oxidation by OH radical together with O_3 in the presence of a few ppb NO_x have been investigated by Yan et al. (Yan et al., 2020). We revisited the data of one 4.5 ppb NO_x experiment and found that $C_{4,5}$ fragmented peaks only accounted for ~ 4.5 % of total products (Fig. R2). In addition, the DBE values of most $C_{4,5}$ fragments are larger than 2, whereas the highest DBE values of IP OOMs in this study is only 2 (Fig. 3). Thus, these fragments almost have no interference with the classification of IP OOMs. Furthermore, the total concentration of MT OOMs in this study is also much lower than IP OOMs. Therefore, a negligible fraction of IP OOMs could raise from fragmented MT OOMs by misclassification.

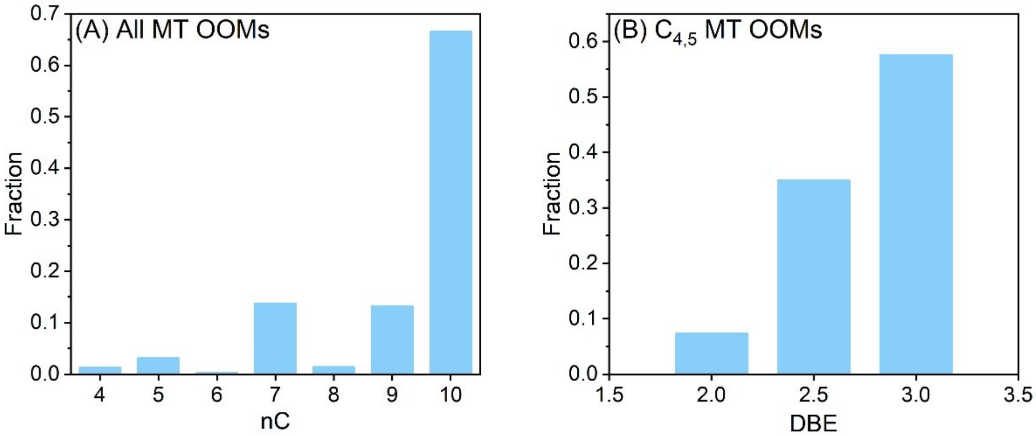

Figure R2. (A) Carbon distribution of all monoterpene oxidation products, and (B) DBE distribution of $C_{4,5}$ monoterpene oxidation products formed by OH radical oxidation together with ozonolyis in previous experiment (Yan et al., 2020). The experiment was conducted under 278 K and the NO_x level was 4.5 ppb.

5. Fig. 3, considering nitrate-CIMS does not detect OOM with low O number, are the OOM with nO_{eff}<=4 mostly organic nitrates?

Response: Yes. Most of $nO_{eff} \leq 4$ OOMs are organic nitrates.

The nitrogen number distributions of OOMs with $nO_{eff} \leq 4$ in four seasons are shown in Fig. R3 (A). It can be found that most OOM molecules contain one or more nitrogen atoms, and they are most likely organic nitrates. Besides, around 11 – 17 % of $nO_{eff} \leq 4$ OOMs contain no nitrogen atom, and most $nO_{eff} \leq 4$ and nN = 0 OOMs possess 4 oxygen atoms (Fig. R3 (B)).

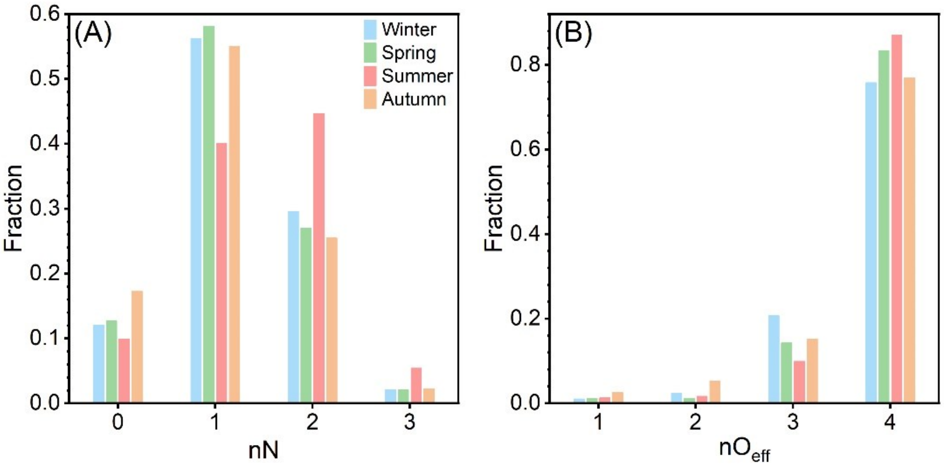

Figure R3. (A) Distribution of nitrogen number (nN) for OOMs with number of effective oxygen no larger than 4 ($nO_{eff} \leq 4$). (B) Distribution of effective oxygen number (nO_{eff}) for OOMs with $nO_{eff} \leq 4$ and nN = 0. The light blue, green, red and orange bars denote winter, spring, summer and autumn, respectively.

6. Fig. 5, it is not completely clear how the spectral profiles are obtained.

Response: In each subplot of Fig. 5, Fig. 7 and Fig. 9, the fraction of each compound is calculated via dividing its concertation by the corresponding total concentration of isoprene OOMs, monoterpene OOMs, aromatic OOMs or aliphatic OOMs.

To clarify this consideration, the captions of Fig. 5, Fig. 7 and Fig. 9 have been modified as follows:

"The fraction of each compound is calculated as the ratio of its concentration to the total concentration of IP OOMs." (Line 344 – 345, Page 13 for Fig. 5)

"The fraction of each compound is calculated as the ratio of its concentration to the total concentration of MT OOMs." (Line 372 – 373, Page 15 for Fig. 7)

"The fraction of each compound is calculated as the ratio of its concentration to the total concentration of aromatic OOMs ((A) to (D)) or aliphatic OOMs ((E) to (H))." (Line 432 – 433, Page 18 for Fig. 9)

7. L262-264, Fig. 5, and Fig.7, analyzing day and night MS spectra separately and plotting the diurnal variation for IP-OOM and MT-OOM may be helpful to estimate the relative contribution of nitrate OOM from NO_x termination and NO_3 radical.

Response: Thank you very much for your suggestions.

The high resolution mass spectra of measured OOMs during day and night are plotted in Fig. R4. It can be found that although the concentrations of OOMs during the night are typically lower than during the day, the overall distributions and patterns of the mass spectra are very similar. Besides, there is almost no peak that is unique for day or night. Therefore, the it is not easy to determine the contribution of NO_3 radical and NO_x termination to nitrate OOM formation based on mass spectra.

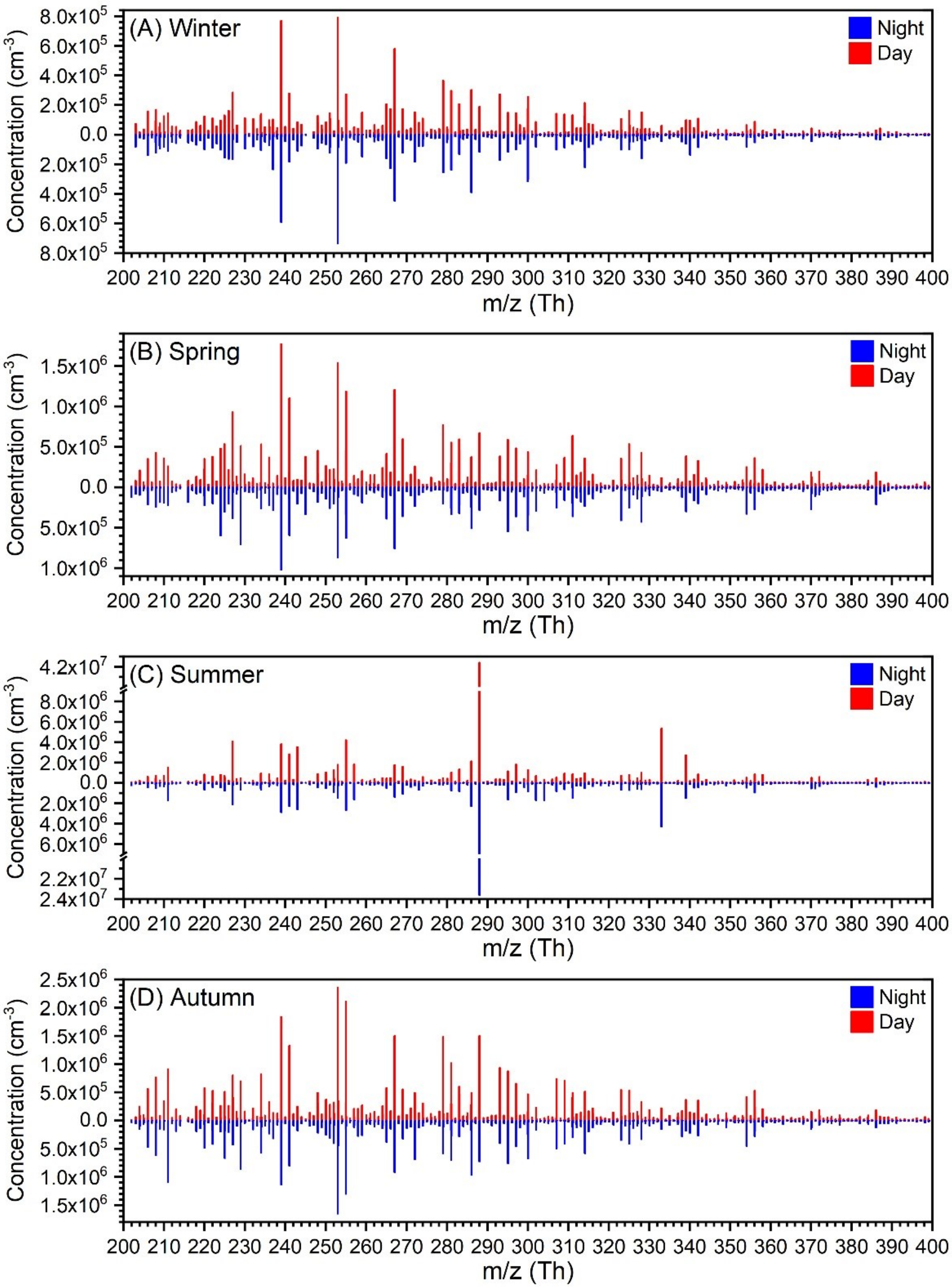

Figure R4. High resolution mass spectrum of measured OOM species during daytime (08:00 – 16:00) and nighttime (20:00 – 04:00 next day) for **(A)** winter, **(B)** spring, **(C)** summer and **(D)** autumn. Red and blue sticks denote datasets from day and night respectively.

As suggested, we further turn to the diurnal variation analysis of IP and MT OOMs. During summertime, each IP or MT OOM can be classified into one of the three types: a. the one with distinct daytime peak; b. the one with day and night dual peaks, and c. the one with elevated concentration at night. Fig. R5 shows the diurnal variations of typical IP and MT OOMs belonging to the above three groups, and **Table R1** summarizes the OOM formulae in each group.

For OOMs with only daytime peaks, they are primarily formed during the day. Some CHON and $CHON_2$ IP-OOMs belong to this group (Table R1), suggesting that they are likely produced from OH initiation followed by NO_x termination. For OOMs with only nighttime peaks, the nighttime chemistry should be their main sources. Only a few IP and MT OOMs containing nitrogen atoms are in this category ($C_5H_9O_4N$, $C_5H_9O_5N$, $C_5H_9O_8N$, $C_5H_{10}O_9N_2$ and $C_{10}H_{15}O_{10}N$). And they should be primarily formed via NO_3 radical oxidation. Besides, their concentration during the day are not zero, suggesting that OH initiation also have contribution to their daytime formation. For OOMs with day and night dual peaks, they have both daytime and nighttime sources. Those OOMs are CHON IP-OOMs, CHON MT-OOMs and $CHON_2$ MT-OOMs. They could be formed from both NO_3 radical oxidation and OH initiation followed by NO_x termination. It should be noted that the diurnal variations of OOMs are also influenced by the boundary layer dynamics and precursor levels. During the night, precursor VOCs, oxidants as well as OOMs should be concentrated by the low boundary layer height and the weak atmospheric diffusion capacity. Therefore, detailed analysis of OOM formation pathway should include the information of boundary layer dynamics and precursor VOCs, but this is out of the scope of current study and we will get into more details in future work.

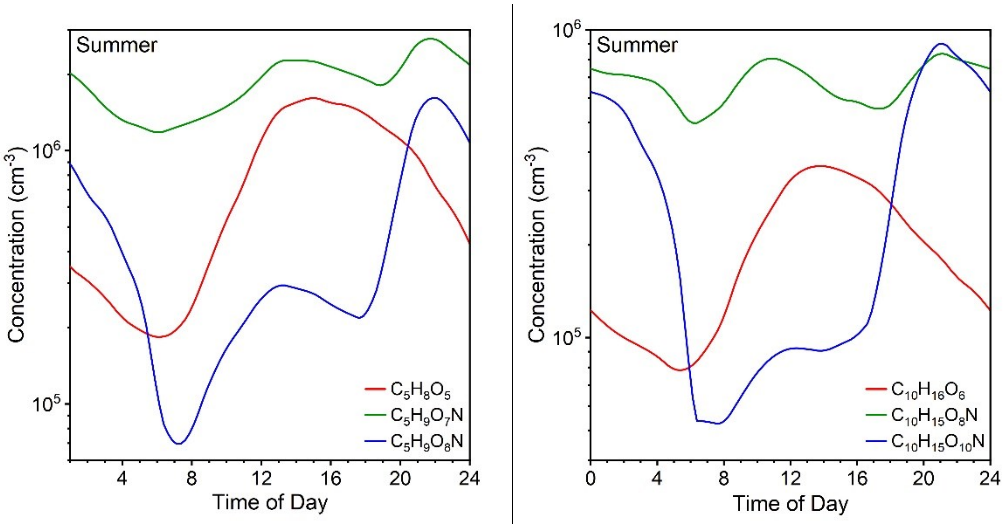

Figure R5. Diurnal variations of typical IP and MT OOMs during summertime. $C_5H_8O_5$ and $C_{10}H_{16}O_6$ only have daytime peak. $C_5H_9O_7N$ and $C_{10}H_{15}O_8N$ possess day and night dual peaks. $C_5H_9O_8N$ and $C_{10}H_{16}O_{10}N$ only have nighttime peak.

Table R1. Formulae of IP and MT OOMs with daytime peak, day-night dual peaks and nighttime peaks in summer.

Daytime Peak		Day-Night Dual Peaks		Nighttime Peak	
IP OOMs	MT OOMs	IP OOMs	MT OOMs	IP OOMs	MT OOMs
$C_4H_8O_6$	$C_{10}H_{14}O_5$	**$C_5H_9O_7N$**	$C_{10}H_{13}O_7N$	$C_5H_9O_4N$	**$C_{10}H_{15}O10N$**
$C_5H_8O_4$	**$C_{10}H_{14}O_6$**	$C_5H_{11}O_7N$	$C_{10}H_{13}O_8N$	$C_5H_9O_5N$	
$C_5H_8O_5$	$C_{10}H_{14}O_7$		$C10H_{13}O_9N$	**$C_5H_9O_8N$**	
$C_5H_8O_6$	$C_{10}H_{16}O_5$		$C_{10}H_{13}O_{10}N$	$C_5H_{10}O_9N_2$	
$C_5H_{10}O_3$	$C_{10}H_{16}O_6$		$C_{10}H_{15}O_7N$		
$C_5H_{10}O_5$	$C_{10}H_{16}O_7$		**$C_{10}H_{15}O_8N$**		
$C_4H_7O_6N$	$C_{10}H_{18}O_5$		$C_{10}H_{15}O_9N$		
$C_5H_9O_6N$	$C_{10}H_{18}O_6$		$C_{10}H_{17}O_7N$		
$C_5H_9O_{10}N$			$C_{10}H_{17}O_8N$		
$C_5H_{11}O_9N$			$C_{10}H_{17}O_9N$		
$C_4H_8O_{10}N_2$			$C_{10}H_{12}O_9N_2$		
$C_5H_{10}O_6N_2$			$C_{10}H_{14}O_{10}N_2$		
$C_5H_{10}O_8N_2$			$C_{10}H_{16}O_{10}N_2$		
$C_5H_9O_{10}N_3$					

Furthermore, for one specific OOM, its diurnal variation may also change in different seasons (Fig. R6). For example, $C_5H_9O_7N$ and $C_{10}H_{15}O_8N$ have day and night dual peaks in summer and spring, while only possess distinct daytime peaks in winter and autumn, suggesting that the their NO_3 radical chemistry plays more important role in summer and spring. Similarly, $C_5H_9O_8N$ and $C_{10}H_{16}O_{10}N$ have higher concentration at night in summer, while this is not all the case for other three seasons.

In summary, the relative contribution of NO_3 radical oxidation and NO_x termination to nitrate OOM formation varies for different OOMs and changes with seasons. Further binPMF analysis, as the work done by Liu et al. (Liu et al., 2021) where nighttime factors take ~ 30 % of total OOM concentration, may help to de-convolute a more accurate contribution.

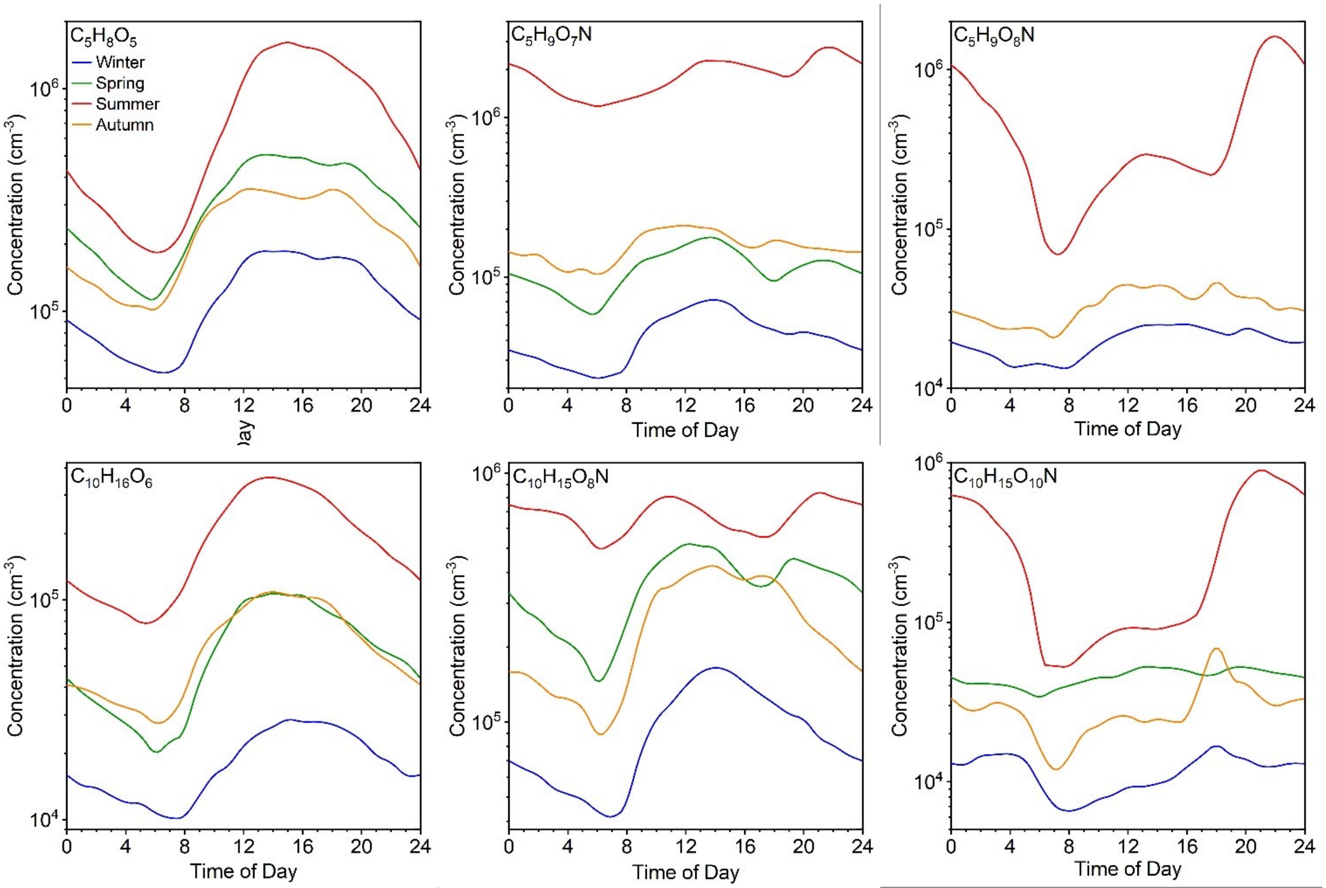

Figure R6. Diurnal variations of typical IP ($C_5H_8O_5$, $C_5H_9O_7N$ and $C_5H_9O_8N$) and MT OOMs ($C_{10}H_{16}O_6$, $C_{10}H_{15}O_8N$ and $C_{10}H_{16}O_{10}N$) in four seasons.

8. L403-405, why CHO accounts for so low fraction compared to other OOM classes?

Response: The reason is not fully understood. The lowest fraction of CHO aliphatic OOMs compared with other OOM classes is probably caused by the highest branching ratio of aliphatic RO_2 - NO_x reaction forming $CHON_x$ species. However, as there the $RO_2 + NO_x$ branching ratios of many OOM molecules are lacking, this hypothesis needs further validation by well controlled chamber experiments.

9. Fig. 11, how the volatility was calculated? As volatility highly depends on the method to derive it, it would be helpful to clarify and maybe add a short discussion on the influence of the methods adopted.

Response: Thanks a lot for pointing out that. The method for estimating OOM volatility was provided in Sect. S2 as follows:

"Detailed structure information of OOMs in real atmosphere is still unknown, therefore, the volatility of each OOM molecule was estimated based on a parameterization using numbers of different atoms (Donahue et al., 2011). For the oxidation products from monoterpenes, previous studies show that except from hydroxyl (-OH), carbonyl (=O) and carboxyl (-O(=O)H) groups, hydroperoxide (-OOH) also takes a large portion (Tröstl et al., 2016;Stolzenburg et al., 2018). Then by assuming that all nitrogen atoms exist as organonitrate groups ($-ONO_2$), the saturation mass concentration of OOM molecule at 300 K can be given as follows (Mohr et al., 2019):

$$\log_{10}C^*(300K) = (25 - nC) \cdot bC - (nO - 3nN) \cdot bO - 2 * \left[\frac{(nO - 3nN) \cdot nC}{nC + nO - 3nN}\right] \cdot bCO - nN \cdot bN \quad (1)$$

where nC, nO and nN are the numbers of carbon, oxygen, and nitrogen in each molecule respectively, and bC=0.475, bO=0.2, bCO=0.9, and bN=2.5. For oxidation products from aromatics, the work of Wang et al. shows that they possess more hydroxyl and carbonyl groups as well as less hydroperoxides, and that their estimated saturation concentrations suggested by Donahue et al. (Donahue et al., 2011) match well with the experiment ones (Wang et al., 2020). Therefore, for those non-monoterpene OOMs, the estimation from Donahue et al. was applied:

$$\log_{10}C^*(300K) = (25 - nC) \cdot bC - nO_{eff} \cdot bO - 2 * \left(\frac{nC \cdot nO_{eff}}{nC + nO_{eff}}\right) \cdot bCO \quad (2)$$

where nC, nO_{eff} and nN are the numbers of carbon, effective oxygen and nitrogen in each molecule separately, and bC=0.475, bO=2.3, and bCO=-0.3.

The temperature dependence of C^* is given by the Clausius-Clapeyron equation (Epstein et al., 2010;Donahue et al., 2012), which we can be approximated as:

$$\log_{10}C^*(T) = \log_{10}C^*(300K) + \frac{\Delta H_{vap}}{R\ln(10)}\left(\frac{1}{300} - \frac{1}{T}\right) \quad (3)$$

where the evaporation enthalpy ΔH_{vap} can be linked with $\log_{10}C^*(300K)$ according to the following equation:

$$\Delta H_{vap}[kJ\ mol^{-1}] = -5.7 \cdot \log_{10}C^*(300K) + 129 \quad (4)$$

After the temperature related saturation concentrations were calculated, OOMs were then grouped into different bins based on the volatility basis set (VBS) (Donahue et al., 2006), and further classified as ELVOCs (extremely low volatility organic compounds), LVOCs (low volatility organic compounds), SVOCs (semi-volatile organic compounds), IVOCs (intermediate volatility organic compounds) and VOCs (volatile organic compounds) according to their volatilities (Donahue et al., 2012)."

We also modified one sentence in the revised manuscript to refer to this volatility calculation.

"Therefore, we estimate the volatility of source-classified OOMs (detailed method can be found in Sect. S3) and summarize the results in Fig. 10." (Line 445 – 446, Page 19)

As for the volatility calculation method, it is true that the derived OOM volatility may vary among different methods. Volatility parameterization based on numbers of different atoms originated from the work of Donahue (Donahue et al., 2011). This study gave a good volatility estimation for OOMs which only contain carbon, hydrogen and nitrogen atoms, and meet the requirements of containing mostly hydroxyl, carbonyl and carboxyl groups and possessing equal fraction of hydroxyl and carbonyl.

With deeper understanding of monoterpene oxidation mechanism during the past decade, many studies have found that hydroperoxide is also a key functional group of monoterpene oxidation products (Ehn et al., 2014;Jokinen et al., 2014;Praplan et al., 2015;Berndt et al., 2016). Based on the proposed structures of those products, the group-contribution method SIMPOL could be applied to calculate the volatilities of monoterpene-derived OOMs. And the results were further used for revising the original volatility parameterization (Tröstl et al., 2016;Stolzenburg et al., 2018;Mohr et al., 2019;Bianchi et al., 2019). And therefore, the volatility estimation of monoterpene OOMs based on Eq. 1 should be pretty robust and has the least uncertainty compared with other types of OOMs.

For aromatic OOMs, the volatility estimation according to Eq. 2 was also evaluated by Wang et al. (Wang et al., 2020). In this work, the oxidation experiments of toluene and naphthalene by OH radical were performed under conditions similar to typical urban environments. Results showed that this equation works well for toluene dimers, naphthalene monomers and naphthalene dimers, while overestimates the volatility a little bit for toluene monomers. In our study, it is likely that most aromatic OOMs are in the form of monomers. And thus, the values of $\log_{10}C^*$ for aromatic OOMs derived from Eq. (2) might be overestimated slightly.

The chemical pathways of atmospheric isoprene oxidation have been investigated for years. Early studies showed that carbonyl, hydroxyl and organonitrate groups are the main functional groups of isoprene OOMs (Lee et al., 2014;Schwantes et al., 2015). In recent years, some studies found that hydroperoxide could also be formed through the process of intramolecular H-shift (Wang et al., 2018;Zhao et al., 2021;Wu et al., 2021). However, different from the stable hydroperoxides on monoterpene OOMs, some hydroperoxides on isoprene OOMs are unstable and may undergo fragmentation (Teng et al., 2017). Besides, this formation of hydroperoxides tend to occur under low-NO_x or experimentally design conditions (D'Ambro et al., 2017;Zhao et al., 2021;Wu et al., 2021). Therefore, the fraction of hydroperoxide groups on isoprene OOMs could not be taken directly from experimental results. Fortunately, the work of Xu et al. (Xu et al., 2021) provided us valuable information of observed isoprene OOMs in Nanjing, one of the Chinese megacities. Results showed that there is large fraction of organonitrate groups and probably small fraction of hydroperoxide groups for isoprene OOMs formed under megacity atmosphere. And this is the reason why we didn't apply the volatility parameterization from monoterpene OOMs, which contain large fraction of hydroperoxides, to isoprene OOMs. In addition, the work of Wu et al. (Wu et al., 2021) estimated the volatility of isoprene nitrates by comparing the difference between two sets of experiments with and without seed aerosol addition. But as seed aerosols inevitably brought in heterogeneous reactions on the surface and liquid phase reactions in the particle phase, this method seems not suitable for volatility acquisition. Future thermal desorption experiments like the one conducted by Wang et al. (Wang et al., 2020) may give better estimation.

For aliphatic OOMs, direct volatility parameterization has been lacking, and only few studies proposed its formation pathways. Conventional knowledge suggests that the oxidation products from alkanes as well as alkenes mainly contain carbonyl, hydroxyl and organonitrate groups (Ziemann, 2011), while possibilities still remain for the formation of hydroperoxides (Rissanen et al., 2014;Rissanen, 2018;Wang et al., 2021). Yet, the lack of mechanism on aliphatic OOM formation under urban-related atmospheric conditions hampers the understanding of aliphatic OOM structures. Thus, we are not able to decide whether Eq. (1) or Eq. (2) is more suitable for them.

To solve this problem, we calculated aliphatic OOM volatility with both methods the results were summarized in Fig. S2. Although some difference appears for detailed volatility distribution, the concentrations of condensable aliphatic OOMs (ELVOCs and LVOCs) based on Eq. (1) and Eq. (2) are very consistent. And therefore, the contribution of aliphatic OOMs to SOA condensation growth will not be influenced too much by the method chosen. In this study, we finally use Eq. (2) to calculate the volatility of aliphatic OOMs.

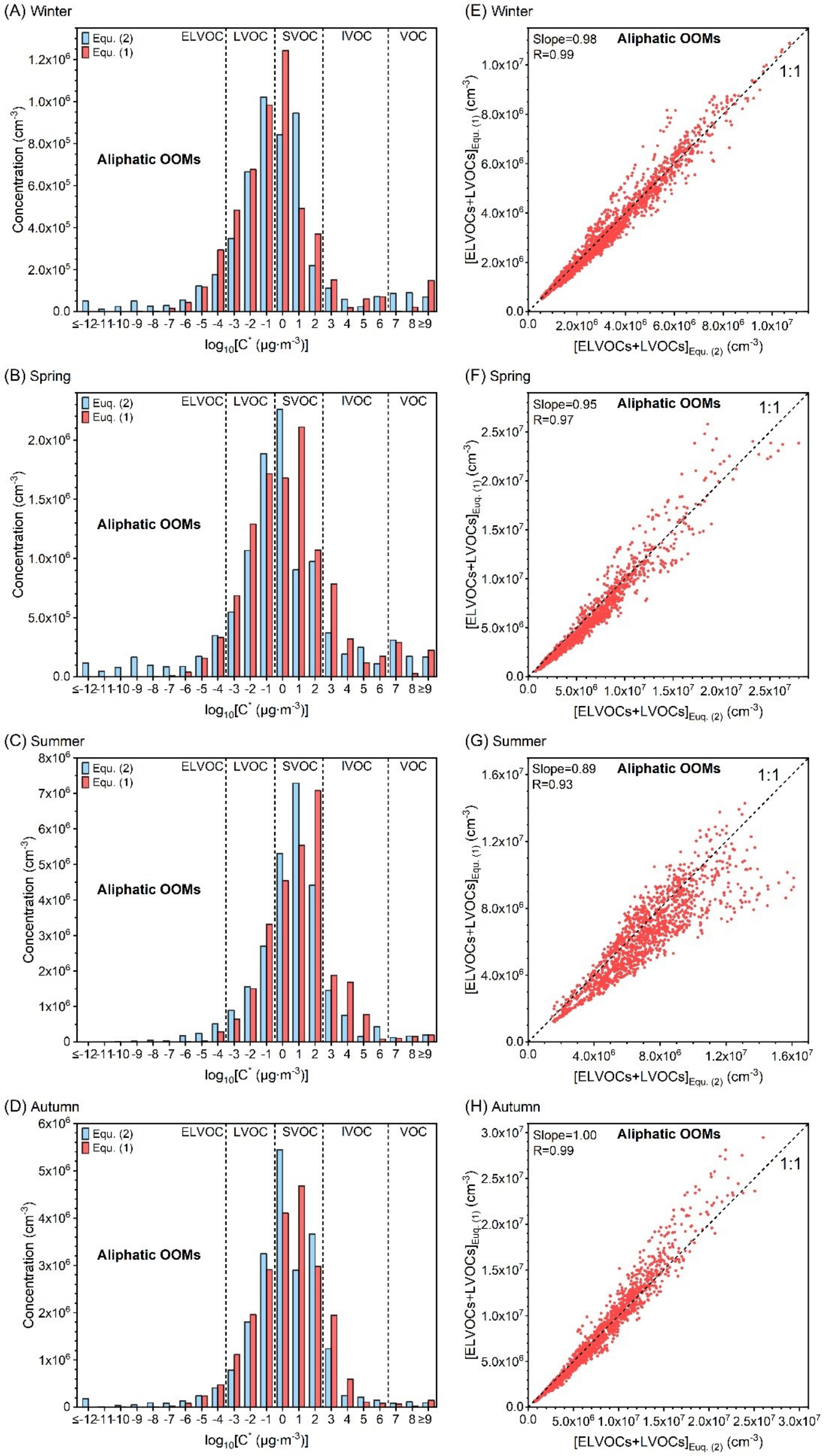

(A) Winter
(B) Spring
(C) Summer
(D) Autumn
Equ. (2)
Equ. (1)
ELVOC
LVOC
SVOC
IVOC
VOC
Aliphatic OOMs
Concentration (cm^{-3})
$\log_{10}[C^*$ (μg·m^{-3})]
≤-12 -11 -10 -9 -8 -7 -6 -5 -4 -3 -2 -1 0 1 2 3 4 5 6 7 8 ≥9
(E) Winter
Slope=0.98
R=0.99
(F) Spring
Slope=0.95
R=0.97
(G) Summer
Slope=0.89
R=0.93
(H) Autumn
Slope=1.00
R=0.99
1:1
[ELVOCs+LVOCs]$_{\text{Equ. (1)}}$ (cm^{-3})
[ELVOCs+LVOCs]$_{\text{Equ. (2)}}$ (cm^{-3})

Figure S2. (A) - (D) Estimated aliphatic OOM volatility distribution derived from two parameterization methods for four season. **(E) - (F)** Comparison of aliphatic OOM concentrations belonging to ELVOCs and LVOCs between two parameterization methods for four seasons. In Fig. (E) to (F), the slopes of least-square linear fit and Pearson coefficients are also listed.

And to clarify this consideration, we added Fig. S2 and the above discussion in the revised supplement as Sect. S4 (Line 62 – 107, Page 3 – 4).

10. L493, "the dominant formation pathways of OOMs stay the same during the year", it might be easier to follow to add "…each OOM stay constant during the year", otherwise it would sound that all OOM are formed in the same pathways.

Response: Thanks a lot for your suggestions and we rewrote this sentence as follows:

"indicating that the dominant formation pathways of each source-classified OOMs stay constant during the year". (Line 503, Page 21)

Technical comments:

1. L173, in Fig. 1, "nO=10" or "nC=10?

Response: Yes, thank a lot. We have corrected this error in Fig. 1.

2. Fig. 3, the order of the legend is not consistent with the order of appearance. It might be easier to follow by keeping it consistent. And there is no legend for light blue.

Response: Yes, thank you very much for your suggestion. We have modified the sequence of the legend in Fig. 3, making it consistent with the appearance order of four seasons.

What do you mean "light blue"? There are only blue bars with diagonal lines and filled colors, and no light blue ones.

3. L443, a space is missing before "94 %".

Response: Thank a lot. We modified this in the revised manuscript. (now Line 455, Page 19)

REFERENCES

Berndt, T., Richters, S., Jokinen, T., Hyttinen, N., Kurtén, T., Otkjær, R. V., Kjaergaard, H. G., Stratmann, F., Herrmann, H., Sipilä, M., Kulmala, M., and Ehn, M.: Hydroxyl radical-induced formation of highly oxidized organic compounds, Nature Communications, 7, 13677, 10.1038/ncomms13677, 2016.

Bernhammer, A. K., Fischer, L., Mentler, B., Heinritzi, M., Simon, M., and Hansel, A.: Production of highly oxygenated organic molecules (HOMs) from trace contaminants during isoprene oxidation, Atmos. Meas. Tech., 11, 4763-4773, 10.5194/amt-11-4763-2018, 2018.

Bianchi, F., Kurten, T., Riva, M., Mohr, C., Rissanen, M. P., Roldin, P., Berndt, T., Crounse, J. D., Wennberg, P. O., Mentel, T. F., Wildt, J., Junninen, H., Jokinen, T., Kulmala, M., Worsnop, D. R., Thornton, J. A., Donahue, N., Kjaergaard, H. G., and Ehn, M.: Highly Oxygenated Organic Molecules (HOM) from Gas-Phase Autoxidation Involving Peroxy Radicals: A Key Contributor to Atmospheric Aerosol, Chemical Reviews, 119, 3472-3509, 10.1021/acs.chemrev.8b00395, 2019.

D'Ambro, E. L., Møller, K. H., Lopez-Hilfiker, F. D., Schobesberger, S., Liu, J., Shilling, J. E., Lee, B. H., Kjaergaard, H. G., and Thornton, J. A.: Isomerization of Second-Generation Isoprene Peroxy Radicals: Epoxide Formation and Implications for Secondary Organic Aerosol Yields, Environmental Science & Technology, 51, 4978-4987, 10.1021/acs.est.7b00460, 2017.

Donahue, N. M., Robinson, A. L., Stanier, C. O., and Pandis, S. N.: Coupled Partitioning, Dilution, and Chemical Aging of Semivolatile Organics, Environmental Science & Technology, 40, 2635-2643, 10.1021/es052297c, 2006.

Donahue, N. M., Epstein, S. A., Pandis, S. N., and Robinson, A. L.: A two-dimensional volatility basis set: 1. organic-aerosol mixing thermodynamics, Atmos. Chem. Phys., 11, 3303-3318, 10.5194/acp-11-3303-2011, 2011.

Donahue, N. M., Kroll, J. H., Pandis, S. N., and Robinson, A. L.: A two-dimensional volatility basis set – Part 2: Diagnostics of organic-aerosol evolution, Atmos. Chem. Phys., 12, 615-634, 10.5194/acp-12-615-2012, 2012.

Ehn, M., Kleist, E., Junninen, H., Petäjä, T., Lönn, G., Schobesberger, S., Dal Maso, M., Trimborn, A., Kulmala, M., Worsnop, D. R., Wahner, A., Wildt, J., and Mentel, T. F.: Gas phase formation of extremely oxidized pinene reaction products in chamber and ambient air, Atmos. Chem. Phys., 12, 5113-5127, 10.5194/acp-12-5113-2012, 2012.

Ehn, M., Thornton, J. A., Kleist, E., Sipilä, M., Junninen, H., Pullinen, I., Springer, M., Rubach, F., Tillmann, R., Lee, B., Lopez-Hilfiker, F., Andres, S., Acir, I.-H., Rissanen, M., Jokinen, T., Schobesberger, S., Kangasluoma, J., Kontkanen, J., Nieminen, T., Kurtén, T., Nielsen, L. B., Jørgensen, S., Kjaergaard, H. G., Canagaratna, M., Maso, M. D., Berndt, T., Petäjä, T., Wahner, A., Kerminen, V.-M., Kulmala, M., Worsnop, D. R., Wildt, J., and Mentel, T. F.: A large source of low-volatility secondary organic aerosol, Nature, 506, 476-479, 10.1038/nature13032, 2014.

Epstein, S. A., Riipinen, I., and Donahue, N. M.: A Semiempirical Correlation between Enthalpy of Vaporization and Saturation Concentration for Organic Aerosol, Environmental Science & Technology, 44, 743-748, 10.1021/es902497z, 2010.

Garmash, O., Rissanen, M. P., Pullinen, I., Schmitt, S., Kausiala, O., Tillmann, R., Zhao, D., Percival, C., Bannan, T. J., Priestley, M., Hallquist, A. M., Kleist, E., Kiendler-Scharr, A., Hallquist, M., Berndt, T., McFiggans, G., Wildt, J., Mentel, T., and Ehn, M.: Multi-generation OH oxidation as a source for highly oxygenated organic molecules from aromatics, Atmospheric Chemistry and Physics, 20, 515-537, 10.5194/acp-20-515-2020, 2020.

Jokinen, T., Sipilä, M., Richters, S., Kerminen, V.-M., Paasonen, P., Stratmann, F., Worsnop, D., Kulmala, M., Ehn, M., Herrmann, H., and Berndt, T.: Rapid Autoxidation Forms Highly Oxidized RO_2 Radicals in the Atmosphere, Angewandte Chemie International Edition, 53, 14596-14600, https://doi.org/10.1002/anie.201408566, 2014.

Lee, L., Teng, A. P., Wennberg, P. O., Crounse, J. D., and Cohen, R. C.: On Rates and Mechanisms of OH and O_3 Reactions with Isoprene-Derived Hydroxy Nitrates, The Journal of Physical Chemistry A, 118, 1622-1637, 10.1021/jp4107603, 2014.

Liu, Y., Nie, W., Li, Y., Ge, D., Liu, C., Xu, Z., Chen, L., Wang, T., Wang, L., Sun, P., Qi, X., Wang, J., Xu, Z., Yuan, J., Yan, C., Zhang, Y., Huang, D., Wang, Z., Donahue, N. M., Worsnop, D., Chi, X., Ehn, M., and Ding, A.: Formation of condensable organic vapors from anthropogenic and biogenic volatile organic compounds (VOCs) is strongly perturbed by NO_x in eastern China, Atmos. Chem. Phys., 21, 14789-14814, 10.5194/acp-21-14789-2021, 2021.

Luo, Y., Garmash, O., Li, H., Graeffe, F., Praplan, A. P., Liikanen, A., Zhang, Y., Meder, M., Peräkylä, O., Peñuelas, J., Yáñez-Serrano, A. M., and Ehn, M.: Oxidation product characterization from ozonolysis of the diterpene ent-kaurene, Atmos. Chem. Phys., 22, 5619-5637, 10.5194/acp-22-5619-2022, 2022.

Mohr, C., Thornton, J. A., Heitto, A., Lopez-Hilfiker, F. D., Lutz, A., Riipinen, I., Hong, J., Donahue, N. M., Hallquist, M., Petaja, T., Kulmala, M., and Yli-Juuti, T.: Molecular identification of organic vapors driving atmospheric nanoparticle growth, Nature Communications, 10, 10.1038/s41467-019-12473-2, 2019.

Nie, W., Yan, C., Huang, D. D., Wang, Z., Liu, Y., Qiao, X., Guo, Y., Tian, L., Zheng, P., Xu, Z., Li, Y., Xu, Z., Qi, X., Sun, P., Wang, J., Zheng, F., Li, X., Yin, R., Dallenbach, K. R., Bianchi, F., Petäjä, T., Zhang, Y., Wang, M., Schervish, M., Wang, S., Qiao, L., Wang, Q., Zhou, M., Wang, H., Yu, C., Yao, D., Guo, H., Ye, P., Lee, S., Li, Y. J., Liu, Y., Chi, X., Kerminen, V.-M., Ehn, M., Donahue, N. M., Wang, T., Huang, C., Kulmala, M., Worsnop, D., Jiang, J., and Ding, A.: Secondary organic aerosol formed by condensing anthropogenic vapours over China's megacities, Nature Geoscience, 15, 255-261, 10.1038/s41561-022-00922-5, 2022.

Praplan, A. P., Schobesberger, S., Bianchi, F., Rissanen, M. P., Ehn, M., Jokinen, T., Junninen, H., Adamov, A., Amorim, A., Dommen, J., Duplissy, J., Hakala, J., Hansel, A., Heinritzi, M., Kangasluoma, J., Kirkby, J., Krapf, M., Kürten, A., Lehtipalo, K., Riccobono, F., Rondo, L., Sarnela, N., Simon, M., Tomé, A., Tröstl, J., Winkler, P. M., Williamson, C., Ye, P., Curtius, J., Baltensperger, U., Donahue, N. M., Kulmala, M., and Worsnop, D. R.: Elemental composition and clustering behaviour of α-pinene oxidation products for different oxidation conditions, Atmos. Chem. Phys., 15, 4145-4159, 10.5194/acp-15-4145-2015, 2015.

Richters, S., Herrmann, H., and Berndt, T.: Highly Oxidized RO2 Radicals and Consecutive Products from the Ozonolysis of Three Sesquiterpenes, Environmental Science & Technology, 50, 2354-2362, 10.1021/acs.est.5b05321, 2016.

Rissanen, M. P., Kurtén, T., Sipilä, M., Thornton, J. A., Kangasluoma, J., Sarnela, N., Junninen, H., Jørgensen, S., Schallhart, S., Kajos, M. K., Taipale, R., Springer, M., Mentel, T. F., Ruuskanen, T., Petäjä, T., Worsnop, D. R., Kjaergaard, H. G., and Ehn, M.: The Formation of Highly Oxidized Multifunctional Products in the Ozonolysis of Cyclohexene, Journal of the American Chemical Society, 136, 15596-15606, 10.1021/ja507146s, 2014.

Rissanen, M. P.: NO2 Suppression of Autoxidation–Inhibition of Gas-Phase Highly Oxidized Dimer Product Formation, ACS Earth and Space Chemistry, 2, 1211-1219, 10.1021/acsearthspacechem.8b00123, 2018.

Schwantes, R. H., Teng, A. P., Nguyen, T. B., Coggon, M. M., Crounse, J. D., St. Clair, J. M., Zhang, X., Schilling, K. A., Seinfeld, J. H., and Wennberg, P. O.: Isoprene NO_3 Oxidation Products from the RO_2 + HO_2 Pathway, The Journal of Physical Chemistry A, 119, 10158-10171, 10.1021/acs.jpca.5b06355, 2015.

Stolzenburg, D., Fischer, L., Vogel, A. L., Heinritzi, M., Schervish, M., Simon, M., Wagner, A. C., Dada, L., Ahonen, L. R., Amorim, A., Baccarini, A., Bauer, P. S., Baumgartner, B., Bergen, A., Bianchi, F., Breitenlechner, M., Brilke, S., Buenrostro Mazon, S., Chen, D., Dias, A., Draper, D. C., Duplissy, J., El Haddad, I., Finkenzeller, H., Frege, C., Fuchs, C., Garmash, O., Gordon, H., He, X., Helm, J., Hofbauer, V., Hoyle, C. R., Kim, C., Kirkby, J., Kontkanen, J., Kürten, A., Lampilahti, J., Lawler, M., Lehtipalo, K., Leiminger, M., Mai, H., Mathot, S., Mentler, B., Molteni, U., Nie, W., Nieminen, T., Nowak, J. B., Ojdanic, A., Onnela, A., Passananti, M., Petäjä, T., Quéléver, L. L. J., Rissanen, M. P., Sarnela, N., Schallhart, S., Tauber, C., Tomé, A., Wagner, R., Wang, M., Weitz, L., Wimmer, D., Xiao, M., Yan, C., Ye, P., Zha, Q., Baltensperger, U., Curtius, J., Dommen, J., Flagan, R. C., Kulmala, M., Smith, J. N., Worsnop, D. R., Hansel, A., Donahue, N. M., and Winkler, P. M.: Rapid growth of organic aerosol nanoparticles over a wide tropospheric temperature range, Proceedings of the National Academy of Sciences, 115, 9122, 10.1073/pnas.1807604115, 2018.

Teng, A. P., Crounse, J. D., and Wennberg, P. O.: Isoprene Peroxy Radical Dynamics, Journal of the American Chemical Society, 139, 5367-5377, 10.1021/jacs.6b12838, 2017.

Tröstl, J., Chuang, W. K., Gordon, H., Heinritzi, M., Yan, C., Molteni, U., Ahlm, L., Frege, C., Bianchi, F., Wagner, R., Simon, M., Lehtipalo, K., Williamson, C., Craven, J. S., Duplissy, J., Adamov, A., Almeida, J., Bernhammer, A.-K., Breitenlechner, M., Brilke, S., Dias, A., Ehrhart, S., Flagan, R. C., Franchin, A., Fuchs, C., Guida, R., Gysel, M., Hansel, A., Hoyle, C. R., Jokinen, T., Junninen, H., Kangasluoma, J., Keskinen, H., Kim, J., Krapf, M., Kürten, A., Laaksonen, A., Lawler, M., Leiminger, M., Mathot, S., Möhler, O., Nieminen, T., Onnela, A., Petäjä, T., Piel, F. M., Miettinen, P., Rissanen, M. P., Rondo, L., Sarnela, N., Schobesberger, S., Sengupta, K., Sipilä, M., Smith, J. N., Steiner, G., Tomè, A., Virtanen, A., Wagner, A. C., Weingartner, E., Wimmer, D., Winkler, P. M., Ye, P., Carslaw, K. S., Curtius, J., Dommen, J., Kirkby, J., Kulmala, M., Riipinen, I., Worsnop, D. R., Donahue, N. M., and Baltensperger, U.: The role of low-volatility organic compounds in initial particle growth in the atmosphere, Nature, 533, 527-531, 10.1038/nature18271, 2016.

Wang, M., Chen, D., Xiao, M., Ye, Q., Stolzenburg, D., Hofbauer, V., Ye, P., Vogel, A. L., Mauldin, R. L., Amorim, A., Baccarini, A., Baumgartner, B., Brilke, S., Dada, L., Dias, A., Duplissy, J., Finkenzeller, H., Garmash, O., He, X.-C., Hoyle, C. R., Kim, C., Kvashnin, A., Lehtipalo, K., Fischer, L., Molteni, U., Petäjä, T., Pospisilova, V., Quéléver, L. L. J., Rissanen, M., Simon, M., Tauber, C., Tomé, A., Wagner, A. C., Weitz, L., Volkamer, R., Winkler, P. M., Kirkby, J., Worsnop, D. R., Kulmala, M., Baltensperger, U., Dommen, J., El-Haddad, I., and Donahue, N. M.: Photo-oxidation of Aromatic Hydrocarbons Produces Low-Volatility Organic Compounds, Environmental Science & Technology, 54, 7911-7921, 10.1021/acs.est.0c02100, 2020.

Wang, S., Riva, M., Yan, C., Ehn, M., and Wang, L.: Primary Formation of Highly Oxidized Multifunctional Products in the OH-Initiated Oxidation of Isoprene: A Combined Theoretical and Experimental Study, Environmental Science & Technology, 52, 12255-12264, 10.1021/acs.est.8b02783, 2018.

Wang, Z., Ehn, M., Rissanen, M. P., Garmash, O., Quéléver, L., Xing, L., Monge-Palacios, M., Rantala, P., Donahue, N. M., Berndt, T., and Sarathy, S. M.: Efficient alkane oxidation under combustion engine and atmospheric conditions, Communications Chemistry, 4, 18, 10.1038/s42004-020-00445-3, 2021.

Wu, R., Vereecken, L., Tsiligiannis, E., Kang, S., Albrecht, S. R., Hantschke, L., Zhao, D., Novelli, A., Fuchs, H., Tillmann, R., Hohaus, T., Carlsson, P. T. M., Shenolikar, J., Bernard, F., Crowley, J. N., Fry, J. L., Brownwood, B., Thornton, J. A., Brown, S. S., Kiendler-Scharr, A., Wahner, A., Hallquist, M., and Mentel, T. F.: Molecular composition and volatility of multi-generation products formed from isoprene oxidation by nitrate radical, Atmos. Chem. Phys., 21, 10799-10824, 10.5194/acp-21-10799-2021, 2021.

Xu, Z. N., Nie, W., Liu, Y. L., Sun, P., Huang, D. D., Yan, C., Krechmer, J., Ye, P. L., Xu, Z., Qi, X. M., Zhu, C. J., Li, Y. Y., Wang, T. Y., Wang, L., Huang, X., Tang, R. Z., Guo, S., Xiu, G. L., Fu, Q. Y., Worsnop, D., Chi, X. G., and Ding, A. J.: Multifunctional Products of Isoprene Oxidation in Polluted Atmosphere and Their Contribution to SOA, Geophysical Research Letters, 48, e2020GL089276, https://doi.org/10.1029/2020GL089276, 2021.

Yan, C., Nie, W., Äijälä, M., Rissanen, M. P., Canagaratna, M. R., Massoli, P., Junninen, H., Jokinen, T., Sarnela, N., Häme, S. A. K., Schobesberger, S., Canonaco, F., Yao, L., Prévôt, A. S. H., Petäjä, T., Kulmala, M., Sipilä, M., Worsnop, D. R., and Ehn, M.: Source characterization of highly oxidized multifunctional compounds in a boreal forest environment using positive matrix factorization, Atmos. Chem. Phys., 16, 12715-12731, 10.5194/acp-16-12715-2016, 2016.

Yan, C., Nie, W., Vogel, A. L., Dada, L., Lehtipalo, K., Stolzenburg, D., Wagner, R., Rissanen, M. P., Xiao, M., Ahonen, L., Fischer, L., Rose, C., Bianchi, F., Gordon, H., Simon, M., Heinritzi, M., Garmash, O., Roldin, P., Dias, A., Ye, P., Hofbauer, V., Amorim, A., Bauer, P. S., Bergen, A., Bernhammer, A. K., Breitenlechner, M., Brilke, S., Buchholz, A., Mazon, S. B., Canagaratna, M. R., Chen, X., Ding, A., Dommen, J., Draper, D. C., Duplissy, J., Frege, C., Heyn, C., Guida, R., Hakala, J., Heikkinen, L., Hoyle, C. R., Jokinen, T., Kangasluoma, J., Kirkby, J., Kontkanen, J., Kürten, A., Lawler, M. J., Mai, H., Mathot, S., Mauldin, R. L., Molteni, U., Nichman, L., Nieminen, T., Nowak, J., Ojdanic, A., Onnela, A., Pajunoja, A., Petäjä, T., Piel, F., Quéléver, L. L. J., Sarnela, N., Schallhart, S., Sengupta, K., Sipilä, M., Tomé, A., Tröstl, J., Väisänen, O., Wagner, A. C., Ylisirniö, A., Zha, Q., Baltensperger, U., Carslaw, K. S., Curtius, J., Flagan, R. C., Hansel, A., Riipinen, I., Smith, J. N., Virtanen, A., Winkler, P. M., Donahue, N. M., Kerminen, V. M., Kulmala, M., Ehn, M., and Worsnop, D. R.: Size-dependent influence of NO_x on the growth rates of organic aerosol particles, Science Advances, 6, eaay4945, 10.1126/sciadv.aay4945, 2020.

Zaytsev, A., Koss, A. R., Breitenlechner, M., Krechmer, J. E., Nihill, K. J., Lim, C. Y., Rowe, J. C., Cox, J. L., Moss, J., Roscioli, J. R., Canagaratna, M. R., Worsnop, D. R., Kroll, J. H., and Keutsch, F. N.: Mechanistic study of the formation of ring-retaining and ring-opening products from the oxidation of aromatic compounds under urban atmospheric conditions, Atmos. Chem. Phys., 19, 15117-15129, 10.5194/acp-19-15117-2019, 2019.

Zhao, D., Pullinen, I., Fuchs, H., Schrade, S., Wu, R., Acir, I. H., Tillmann, R., Rohrer, F., Wildt, J., Guo, Y., Kiendler-Scharr, A., Wahner, A., Kang, S., Vereecken, L., and Mentel, T. F.: Highly oxygenated organic molecule (HOM) formation in the isoprene oxidation by NO3 radical, Atmos. Chem. Phys., 21, 9681-9704, 10.5194/acp-21-9681-2021, 2021.

Ziemann, P. J.: Effects of molecular structure on the chemistry of aerosol formation from the OH-radical-initiated oxidation of alkanes and alkenes, International Reviews in Physical Chemistry, 30, 161-195, 10.1080/0144235X.2010.550728, 2011.